Effects of state-selective charge-exchange processes on the He-like spectra from the Alcator C tokamak

T. Kato and K. Masai
National Institute for Fusion Science, Nagoya 464-01, Japan

T. Fujimoto
Department of Engineering Science, Kyoto University, Kyoto 606, Japan

F. Koike
School of Medicine, Kitasato University, Kanagawa 228, Japan

E. Källne
Department of Physics I, The Royal Institute of Technology, S-10044 Stockholm, Sweden

E. S. Marmar and J. E. Rice
Plasma Fusion Center, Massachusetts Institute of Technology, Cambridge, Massachusetts 02139
(Received 2 January 1991)

The effects of a low-energy charge-exchange process between hydrogenlike ions and neutral hydrogen on x-ray spectra of He-like argon ions from the Alcator C tokamak are investigated. Dependences of charge-exchange cross sections on both the principal and angular momentum quantum numbers n and l are estimated from the observed spectra, taking cascade effects into account with the use of a collisional radiative model.

PACS number(s): 52.20.Hv, 34.70.+e, 34.80.Kw, 52.70.La

I. INTRODUCTION

X-ray spectral lines associated with He-like ions have been observed for many tokamak plasmas, and their emission intensities have been discussed in terms of population mechanisms of excited states. In quantitative analysis of the spectra, ionization, excitation, and recombination processes have been taken into consideration, but the charge-exchange process has generally been ignored except for the case of neutral-beam injection. Although the influence of the charge-exchange process on the spectra is mentioned in the discussion of some experiments, only a qualitative account is presented. The charge-exchange process could be important for He-like spectral lines in relation to the population mechanism following the electron capture into higher energy levels. We investigate this process using a collisional radiative model that includes all the possible angular momentum l-state sublevels up to the principal quantum number $n=40$ of the He-like system. We apply this model to the spectra obtained from Alcator C tokamak plasmas [1–3] and derive the n-l distribution of charge-exchange cross sections.

II. X-RAY SPECTRA FROM THE ALCATOR C TOKAMAK

In this section we summarize the results of the experiments on the Alcator C tokamak [1–3]. Our investigation described in the subsequent sections is based on these observations.

Space-resolved x-ray spectra of Ar^{16+} (He-like) were observed from Alcator C tokamak plasmas seeded with Ar gas. In Fig. 1, reproduced from Ref. 1, spectral lines from $n=2$ to 1 transitions, $w(1s^2\,{}^1S-1s2p\,{}^1P)$, $x(1s^2\,{}^1S-1s2p\,{}^3P_2)$, $y(1s^2\,{}^1S-1s2p\,{}^3P_1)$, and $z(1s^2\,{}^1S-1s2s\,{}^3S)$, are shown for three different lines of sight through the plasma; these are at the center (a), and through the points of $d=8.3$ (b) and 11.3 cm (c) off from the center, where d is the shortest distance to the chord of observation from the plasma axis. The limiter radius was 16.5 cm. One can see a drastic change in the spectra from the central chord to the outer ones. The relative intensities of the forbidden line I_z and the intercombination lines I_x and I_y to the resonance line intensity I_w: I_z/I_w, I_x/I_w, and I_y/I_w, increase remarkably towards the outer chords. This relative enhancement could be accounted for by an increasing contribution from radiative recombination to the excited-level populations [3] towards the outer region. The spectrum in Fig. 1(c), however, cannot be accounted for only by the radiative recombination process. The observed intensity ratio of $I_z/(I_x+I_y)=0.9\pm0.2$, is considerably smaller than the value 1.5 expected from radiative recombination. A possible interpretation is that a charge-exchange process between Ar^{17+} (H like) and hydrogen atoms dominates the population of highly excited states, and that the relative enhancement of the intercombination lines results through cascades [1].

X-ray spectra of the transitions $1s^2-1snp$ with $3\leq n\leq\infty$ were also obtained [2]. Figure 2 shows the observed spectra with $7\leq n\leq 13$ through the three chords

$d=$ (a) 3.9 cm, (b) 8.0 cm, and (c) 13.5 cm. As seen in Fig. 2, the transitions from $n=9$ and 10 are enhanced relatively to those from $n=7$ and 8 towards the outer chord. This is regarded as a clear evidence of charge-exchange recombination between Ar^{17+} and neutral hydrogen in the ground state into the levels of $n=9$ and 10 [2,3]. Another observed spectrum corresponding to the highly excited states $n \geq 10$ is shown in Fig. 3, which was obtained for $d=8.3-13.2$ cm. The spectrum in Fig. 3 shows a broad feature from 3.01 to 3.02 Å. A peak at around 3.013 Å corresponds to the transitions from $n \approx 27$ and the shoulder near 3.018 Å to the transition from $n \approx 18$. These enhancement are attributed to electron capture from hydrogen atoms in the excited states with the principal quantum number $n_i=3$ and 2, respectively [2].

III. EFFECT OF CASCADES FOLLOWING CHARGE EXCHANGE RECOMBINATION

We construct a collisional radiative model for He-like ions where the levels of $n \leq 40$ are resolved with different

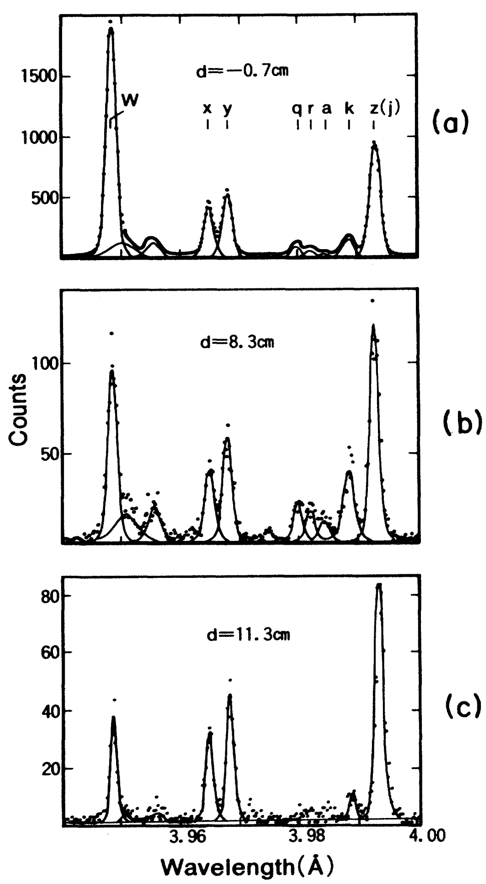

FIG. 1. Observed spectra of $1s^2-1s2l$ transitions in Ar^{16+} from Alcator *C* tokamak for three different chords (from Ref. [1]). *w*, $1s^2\,{}^1S-1s2p\,{}^1P$; *x*, $1s^2-1s2p\,{}^3P_2$; *y*, $1s^2\,{}^1S-1s2p\,{}^3P_1$; *z*, $1s^2-1s2s\,{}^3S$.

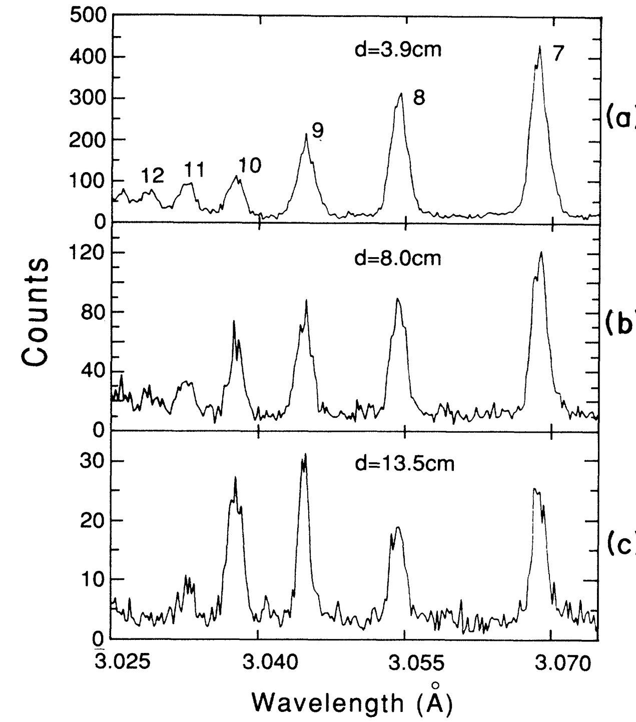

FIG. 2. Observed spectra of $1s^2-1snp$ transitions with $7 \leq n \leq 13$ in Ar^{16+} from Alcator *C* tokamak for three different chords (from Ref. [2]).

angular momentum *l*. All the collisional processes include those among the sublevels are considered as well as the radiative transitions. The total number of levels considered is 1641. In the present study, we include the charge-exchange process

$$Ar^{17+}(1s)+H(n_i) \rightarrow Ar^{16+}(1snl)+H^+ \quad (1)$$

as an additional population mechanism of excited levels.

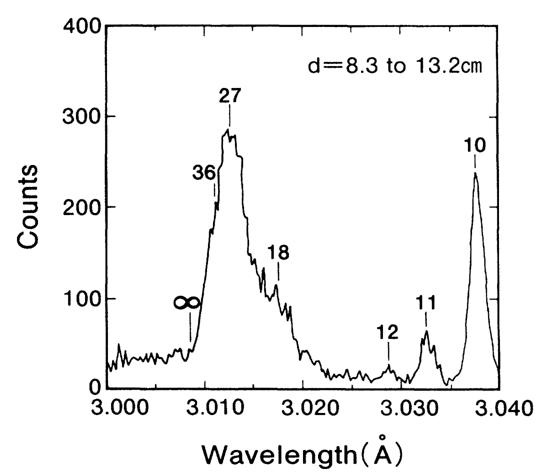

FIG. 3. Observed spectra of $1s^2-1snp$ transitions with $n \geq 10$ in Ar^{16+} from Alcator *C* tokamak (from Ref. [2]).

Adjusting the magnitude of the charge-exchange cross sections, we try to fit the modeled results for line intensities to the experimental data described in the preceding section.

A. The *n*-*l* distribution of the charge-exchange cross section

Abramov, Baryshnikov, and Lisitsa [5] obtained an l distribution w_{nl} for the charge-exchange process based on the Landau-Zener theory with a modification including rotational coupling effects

$$w_{nl}=(2l+1)[(n-1)!]^2/[(n+l)!(n-1-l)!] \ . \qquad (2)$$

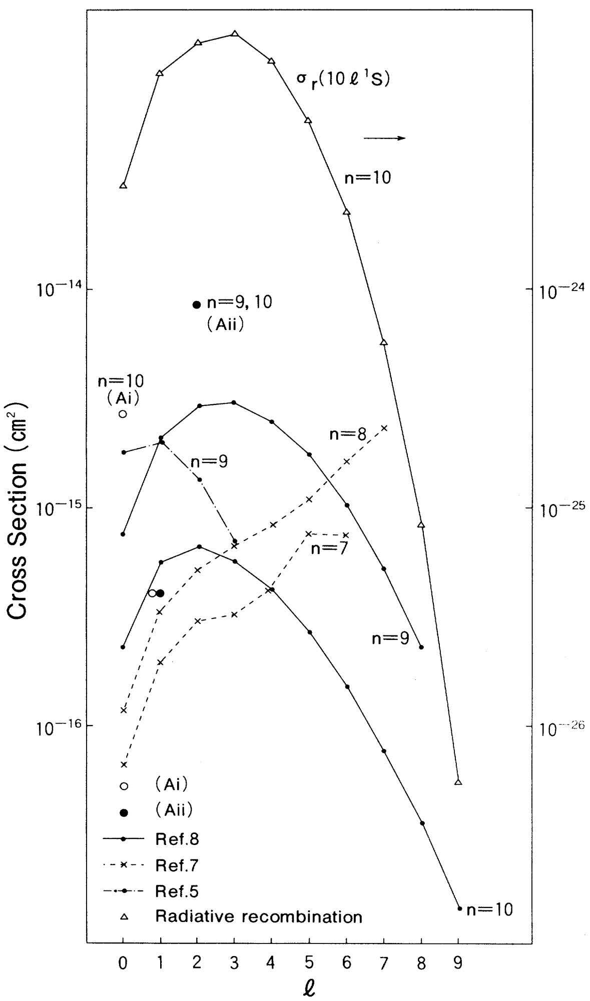

FIG. 4. l distribution of the cross section for the charge transferred electrons at low energies. Solid lines indicate the theoretical results by Koike [8] for $Ar^{17+}+H$ at 0.35 keV/amu, dashed lines from Fritsch and Tawara [7] for $Si^{13+}+H$ at 0.35 keV/amu; dotted-dashed line from Abramov [5] for $A^{17+}+H$ at 0.5 keV/amu. The derived distributions from the spectra are shown by open circles for case (A i) and by closed circles for case (A ii), respectively. The l distribution for the radiative recombination cross section of $n=10$ levels is also shown in the upper part for comparison.

The cross section takes its maximum value 7×10^{-15} cm^2 at around $n=9$ for $H+Ar^{q+}$ collisions with $q=17$ [6]. The l distribution in Eq. (2) for $n=9$ is shown in Fig. 4 by the dotted-dashed line. The n-l distribution for the charge-transfer cross section for $H+Si^{q+}$ collisions was calculated in Ref. 7 with atomic-orbital basis. Their distribution for collisions between H-like silicon (Si^{13+}) and H atoms at 350 eV increases with increasing the l value similarly to the statistical weight, as shown in Fig. 3 by dashed lines. A continuous-energy state model is proposed for charge-transfer processes by Koike [8], whose method is applied to the n-l distribution of the process given by Eq. (1). The cross section at 350 eV takes its maximum at around $l=3$ from his results as indicated in Fig. 4 by solid lines for $n=9$ and 10. Three different theories give quite different distributions. The l distribution for $n=10$ of radiative recombination σ_r at 100 eV is shown in the upper part of Fig. 4 for comparison. The l value that gives the maximum of σ_r increases as the electron energy decreases and as the principal quantum number n increases, but the value does not exceed $l=4$. The points of (A i) and (A ii) in Fig. 4 are the derived values from the spectra and are discussed in Sec. II C.

B. Contribution of radiative recombination by electron collisions

The intensity I_{10} in Fig. 3 is much stronger than those of I_{13} and I_{14}, where I_n means the line intensity of the $1s^2$-$1snp$ transition. Due to convective transport in the plasma, a considerable fraction of highly ionized ions may exist even in the outer regions with the temperature as low as ~300 eV. Ar^{16+} spectra observed from such a plasma exhibit typical characteristics of recombination [3,4]. In fact, as seen in Fig. 3, the recombination continuum is detected at wavelengths shorter than 3.0088 Å which is the ionization limit of the $1s^2$ state. We assign the intensity at the I_{13} location as due to radiative recombination. Then we estimate the upper limit of the electron temperature T_e to be about 500 eV from the observed intensity ratio of $I_{13}/J_{cont}\leq2.8\times10^{-4}$ Å, where J_{cont} represents the continuum intensity in units of photons/Å. The continuum level is taken from the short-wavelength edge of the spectrum. The value 500 eV is reasonable for the electron temperature around $r=11$ cm. From the intensity of I_{13}, the contribution of radiative recombination to the line intensities, $I_{10}-I_{12}$, and $I_{n\geq15}$ is estimated. The resulting intensities are much lower than those observed. On the other hand, the contribution of electron excitation is estimated to be negligibly small since the electron temperature is much lower than the excitation energies.

Thus, the intensity I_{10} is understood to be dominated by direct electron capture through charge exchange with neutral hydrogen. The intensities I_{10} and J_{cont} are written as

$$I_{10}=N(Ar^{17+})N_H(1)\langle\sigma_{CE}(1s10p\,^1P)v\rangle \ , \qquad (3)$$

$$J_{\text{cont}} = N(\text{Ar}^{17+}) N_e \alpha_r (\lambda = 3\ \text{Å}) , \tag{4}$$

where

$$\alpha_r(\lambda\,(\text{Å})) = 3.97 \times 10^{-12} \exp \times (I_z - 12.4/\lambda)\lambda^{-1}[kT_e\ (\text{keV})]^{-3/2} d\lambda \quad (\text{photons/Å})\ \text{cm}^3\text{s}^{-1} \tag{5}$$

is the radiative recombination rate coefficient at wavelength λ (in Å), T_e the electron temperature, $\sigma_{\text{CE}}(1s10p\ ^1P)$ is the charge-exchange cross section to the $1s10p\ ^1P$ state, v the velocity of Ar^{17+} relative to the hydrogen atoms, and N_e and $N_{\text{H}}(1)$ the densities of the electron and the neutral hydrogen in the ground state, respectively. Then the following relation is derived from the observed value $I_{10}/J_{\text{cont}} d\lambda = 8$ where $d\lambda = 1.79 \times 10^{-3}$ Å:

$$\sigma_{\text{CE}}(1s10p\ ^1P) v N_{\text{H}}(1)/N_e = 5.0 \times 10^{-14}\ \text{cm}^3\text{s}^{-1} . \tag{6}$$

For the values of $N_e = 5 \times 10^{13}$ cm^{-3}, $N_{\text{H}}(1) = 10^9$ cm^{-3}, and $v = 2.5 \times 10^7$ cm/s ($T_i = 350$ eV), the cross section $\sigma(1s10p\ ^1P)$ is estimated to be 1.0×10^{-16} cm^2. Assuming the statistical distribution for singlet and triplet states, we obtain $\sigma(1s10p) = 4.0 \times 10^{-16}$ cm^2 which is consistent with the theoretical value [8] (see Fig. 4). But this value changes according to the estimate of the densi-

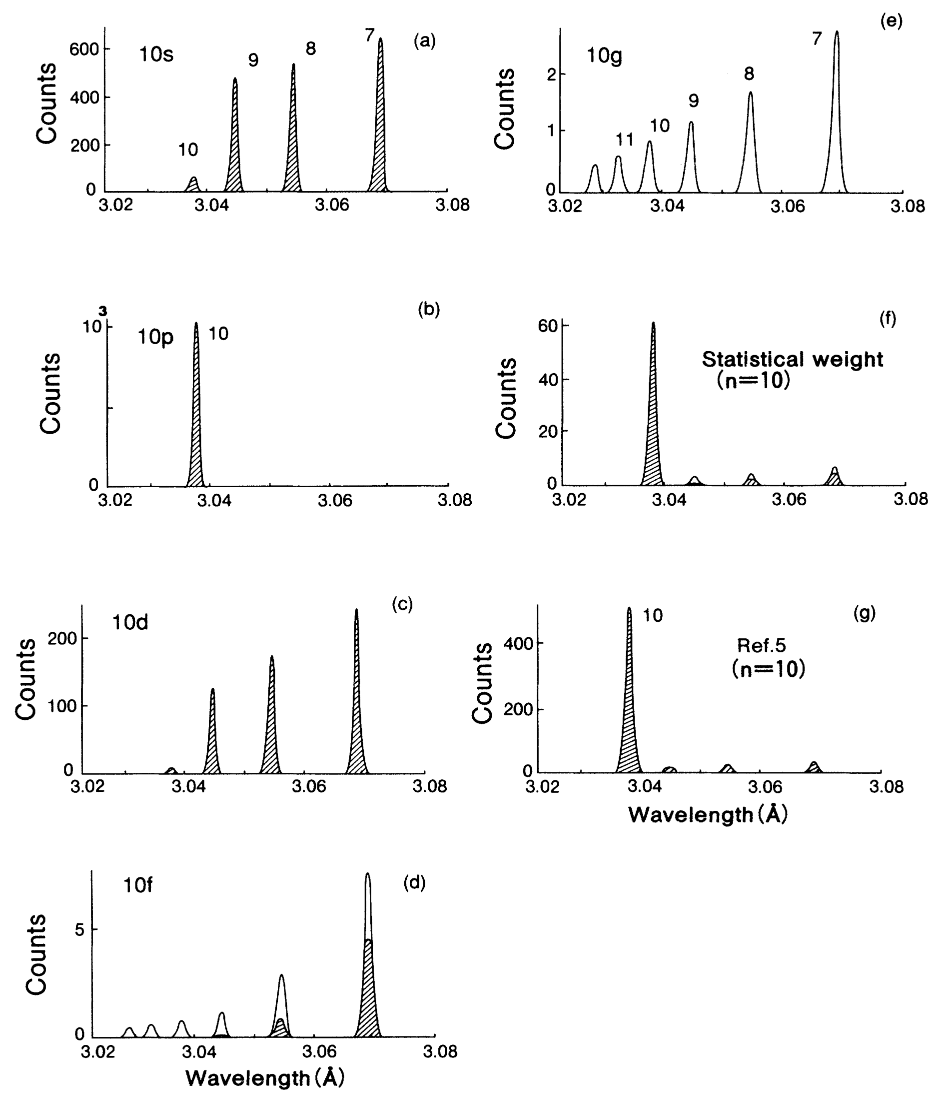

FIG. 5. The modeled spectra for the transitions of $n = 7-12$ due to the charge transfer to the $10l$ selected state are shown for (a) $10s$, (b) $10p$, (c) $10d$, (d) $10f$, and (e) $10g$, respectively. The hatched regions indicate the contribution by charge exchange. The spectrum of (e) is the same as that from only radiative recombination. The spectra with the statistical weight distribution and Eq. (2) are also shown in (f) and (g).

ties of electron and neutral hydrogen as well as of the ion temperature. We discuss only the relative values for the cross section later on.

C. Cascade effect of l distribution on the spectra with $7 \leq n \leq 12$

We now turn to the lines from $n=7-9$ in Fig. 2(c), where the electron temperature is estimated to be about 290 eV. The intensities $I_{n=7-9}$ are also much stronger than $I_{n \geq 11}$, and we assume that this enhancement is attributed to charge-exchange recombination as in the case of I_{10}. However in the present case, it is unlikely that these upper levels are populated entirely by direct capture. Rather, the fact that the intensity I_7 is higher than I_8 strongly suggests some contribution of cascades from $n=10$ and/or 9.

In Fig. 5 we show the modeled results for spectra including charge-exchange recombination for the capture into the $10l$ selected state ($l=1,2,\ldots$) in order to see the effect of the l distribution on the spectra. The charge-exchange recombination rate coefficient is tentatively assumed to be $\alpha_{CE}=5.2\times10^{-6}$ cm^{3}s^{-1}, which is much larger than that of the radiative recombination rate by ten orders of magnitude, in order to see the effect by charge-exchange recombination. The distribution ratio of the singlet state to the triplet one is assumed to be $\frac{1}{3}$ according to their statistical weights. For the case that the electron is captured into the $10s$ state, the cascade effect on $n=7$ and 8 levels is quite large as shown in Fig. 5(a). The contribution by cascades after charge-exchange recombination is indicated by the hatched regions, and the region without hatching is the contribution of radiative recombination. Cascades following capture into the $10p$ state to the lower levels ($n \leq 9$) is very small, since the direct radiative transition from $10p$ to $1s$ is dominant [Fig. 5(b)]. For the case of capture into $10d$, although the cascade is not so large as in the case of $10s$ due to the radiative transitions to the f states, the cascade is very effective [Fig. 5(c)]. Increasing the l values with $f,g,\ldots$, the cascade effect decreases. For the capture into the levels with $l \geq 4$, the cascade contribution is negligibly small and the line emissions are dominated by radiative recombination as shown in Fig. 5(e). Figures 5(f) and 5(g) show the modeled results with the distribution of statistical weight like Ref. 7 and with Eq. (2), respectively. Cascades to the levels $n \leq 9$ are very small compared to the intensity from the transition from $n=10$ for both cases. With the electron density of 5×10^{13} cm^{-3}, the collisional mixing among l levels can be ignored, although the collisional mixing process is included. This effect becomes important for $n>20$.

We consider two extreme cases; (A) I_7 and I_8 are produced only by cascades from the $n=9$ and 10 levels, and (B) I_7 and I_8 are produced mainly by direct capture to the p state.

Case (A): Most of the electrons captured to the $9l$ or $10l$ state flow to lower states ($n=1,2,3$, etc.) through direct radiative transitions and a few percent of electrons flow to the $7p$ state to produce I_7. Electron capture to the s states enhances I_7 and I_8 through cascades most effectively. This results in strong I_z as discussed in the next section. The electron capture to the levels of larger l values such as $9f$ and $9g$ is not efficient in producing the resonance series lines I_7 and I_8. The best candidate to enhance these lines is charge exchange to s and d states. We derive the values of the cross section in order to account for the measured intensities of I_7 and I_8. The cross sections relative to that for the $10p$ state are obtained for (i) $10s$, $9p$, and $9s$ states and (ii) $10d$, $9p$, and $9d$ states.

TABLE I. Relative charge-exchange cross sections for $Ar^{17+}+H(1)\rightarrow Ar^{16+}(nl)+H^{+}$. The cross sections are normalized to $\sigma(1s10p)=4.0\times10^{-16}$ cm^2 in the cases of (A ii) and (B ii).

	$n=7$	$n=8$	$n=9$	$n=10$	Total
			Case (A i)		
s			6.3	6.8	
p			0.95	1.1	
					14.6
			Case (A ii)		
p			1.0	1.0	
d			21.0	21.0	
					44.0
			Case (B i)		
s	2.1	4.3	4.3	2.1	
p	0.2	0.35	1.2	1.1	
					15.6
			Case (B ii)		
p	0.3	0.35	1.2	1.0	
d	2.8	3.3	11.5	10.0	
					33.1

The resulting cross sections for the s and d states are larger by a factor of 5 and one order of magnitude, respectively, than that for the $10p$ state. A part of I_9 is ascribed to the direct capture to the $9p$ state through charge exchange. The relative cross sections thus derived are summarized as cases (A i) and (A ii) in Table I, and the resultant line intensities for I_7-I_{10} are compared with the measurement in Fig. 6, where $T_e=300$ eV, $N_e=5\times10^{13}$ cm^{-3}, $N(\mathrm{Ar}^{17+})/N(\mathrm{Ar}^{16+})=0.02$, and $N_{\mathrm{H}}(1)=8\times10^{8}$ cm^{-3} are assumed. The filled circles and triangles are the modeled results from the cases of (A i) and (A ii), respectively, and the measurements are indicated by the crosses. The contribution of radiative recombination is small compared to charge-exchange recombination as indicated by open circles in Fig. 6. The derived cross sections with the parameters mentioned above are shown in Fig. 4 by circles.

Case (B): The intensities I_7-I_{11} are dominated by direct capture to np states. The intensity difference between I_7 and I_8, however, is to be explained by cascades from $n=9$ and 10. The cross sections deduced under this assumption are listed in Table I for two cases: (i) s and p states and (ii) p and d states. Modeled results of line intensities for (B) are not shown in Fig. 6 since they are nearly the same as for (A).

The observed intensities I_7 and I_8 cannot be reproduced by the distribution given by Refs. [5], [7], and [8] because the cascade contribution to I_7 is too small. The modeled results for line intensities from the distribution by Koike [8] is shown by open triangles in Fig. 6. The dominantly populated final state n_m is given by $2^{1/4}Z^{3/4}$ at low energies which gives $n_m=10$ for $Z=17$. This value is reasonable for our modeled results. We consider that the real values lie between cases (A) and (B).

D. Cascade effects on the spectra for the transitions of $n=2$ to 1

The cascade contribution from the levels of large l value such as d, f, g states enhances the intensity ratio $(I_x+I_y)/I_z$, whereas the cascades from the levels of small l value such as s states reduce this ratio. With increasing l values, the intensity ratio $(I_x+I_y)/I_w$ becomes smaller. In Fig. 7 modeled intensities of I_w, I_x, and I_y normalized to I_z are shown by solid lines for the cases of charge exchange to $n=10$ state with only one of the levels of $l=0$, 1, 2, 3, 4, and 9. The modeled results from radiative recombination only are indicated by circles for 300 eV. The observed values are also plotted as the dashed lines with the electron temperatures [1,3]. The spectra at high temperatures are from the central region of the plasma and dominated mainly by electron impact excitation. The spectra, at lower temperatures below 350 eV, are considered to consist of the two components due to radia-

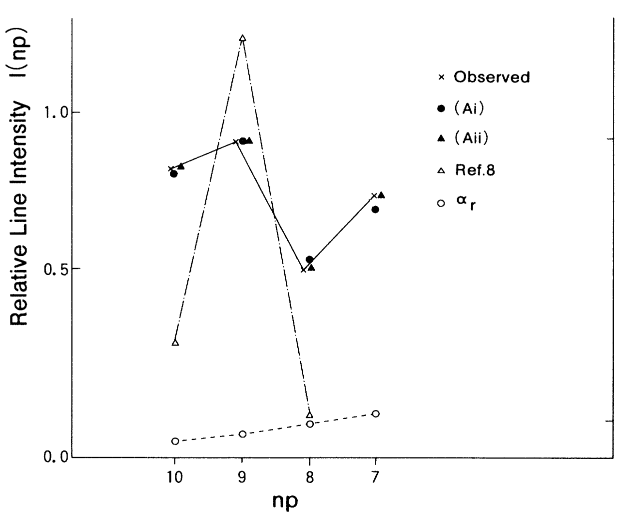

FIG. 6. Line intensities $I(np)$ for $1s^2$-$1snp$ transitions with $7\leq n\leq 10$, where np means the upper state of the transition. The filled circles and triangles are the modeled results for the cases of (A i) and (A ii) in Table I. The crosses indicate the measurement at around 290 eV which corresponds to Fig. 2(c). The open circles show the contribution by radiative recombination. The open triangles are the modeled intensities from the distribution of Ref. [8]. $T_e=350$ eV, $N_e=5\times10^{13}$ cm^{-3}, $N_{\mathrm{H}}=10^{9}$ cm^{-3}, and $N(\mathrm{Ar}^{17+})/N(\mathrm{Ar}^{16+})=0.02$ are taken for calculations.

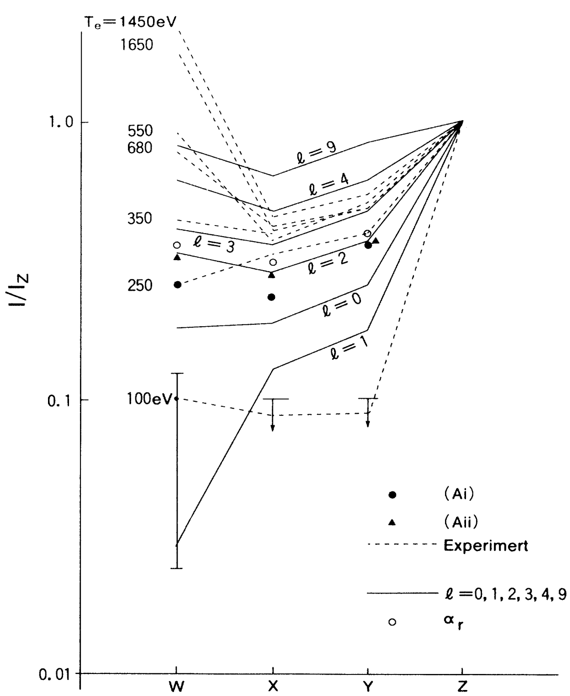

FIG. 7. Intensity ratios of I_w, I_x, and I_y to I_z. The solid lines are the modeled results assuming the charge-exchange recombination to the $10l$ state. Dashed lines are the observed values. The calculated ones by (○), radiative recombination only (●), charge-exchange recombination with the distribution (A i), and (▲), (A ii) in Table I.

tive and charge exchange recombination. It is seen from Fig. 7 that as the temperature decreases, the intensities of w, x, and y decrease. This may indicate the temperature dependence of the l distribution of charge-exchange processes due to the change of the energy of the neutral hydrogen. Capture to the levels $l=3$ is necessary to explain the observed intensity ratios of $(I_x+I_y)/I_z$ for 350 eV when they are compared to the values of the radiative recombination process only (open circles in Fig. 7). The distribution $l=0$ or 1 is most probable for explaining the spectra at 100 and 250 eV. The modeled intensity ratios for case of (A i) and (A ii) in Table I are shown in Fig. 7 by filled circles and triangles. The observed spectrum of 250 eV can be roughly explained by these cross sections.

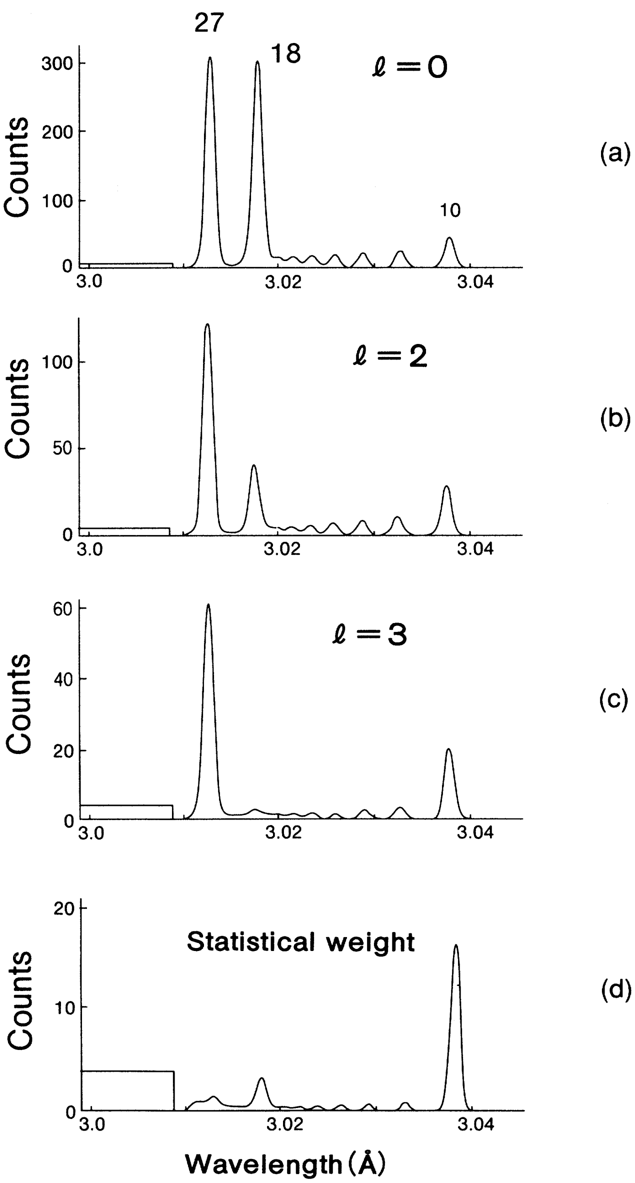

FIG. 8. Modeled spectra for $n \geq 10$ with different l distributions of the charge-exchange cross sections of $\alpha_{CE}(18l)=1.8\times10^{-7}$ and $\alpha_{CE}(27l)=6.9\times10^{-8}$ cm^3s^{-1}. (a) $l=0$, (b) $l=2$, (c) $l=3$, and (d) statistical weight.

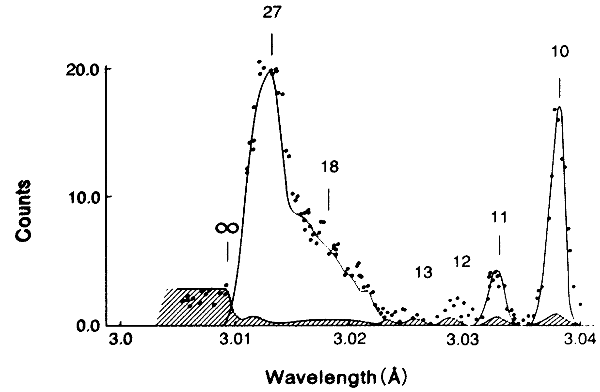

FIG. 9. Modeled spectrum (solid curve) and observed one (points) of $1s^2$-$1snl$ transitions with $n \geq 10$. The hatched regions show the contribution by radiative recombination.

E. Spectra of the transitions with $n \geq 15$

The broad feature for $n \geq 15$ in Fig. 3 is considered to be due to charge exchange between hydrogen atoms in excited states and Ar^{17+} [2]. The electrons are captured to the levels near $n=18$, 27, and 36 by charge exchange with hydrogen in $n_i=2$, 3, and 4, respectively [2,9]. The

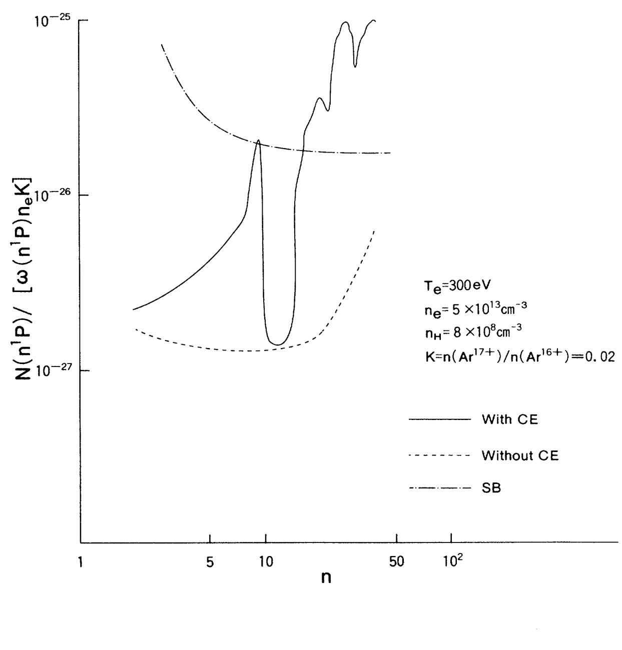

FIG. 10. Boltzmann plot $N(n\,^1P)/[\omega(n\,^1P)n_e k]$ under the condition of $N_e=5\times10^{13}$ cm^{-3}, $T_e=300$ eV, and $k=N(Ar^{17+})/N(Ar^{16+})=0.02$. The modeled one with the charge-exchange cross sections in Tables I and II is given by solid line. The dotted line and dotted-dashed line show the results without charge-exchange recombination and in the Saha-Boltzmann equilibrium, respectively.

TABLE II. Relative charge-exchange cross sections for $Ar^{17+}+H(n_i)\rightarrow Ar^{16+}(nl)+H^+$ ($n_i \geq 2$ and $n \geq 15$). The cross sections are normalized to $\sigma(1s10p)=4.0\times10^{-16}$ cm^2. Numbers in square brackets denote powers of 10.

$n_i=2$		$n_i=3$		$n_i=4$	
15p	4.1[1]	24p	1.4[2]	32p	1.2[2]
16p	5.7[1]	25p	1.5[2]	33p	1.3[2]
17p	6.5[1]	26p	1.6[2]	34p	1.5[2]
18p	6.8[1]	27p	1.8[2]	35p	1.6[2]
19p	6.8[1]	28p	1.6[2]	36p	1.6[2]
20p	6.8[1]	29p	1.5[2]	37p	1.6[2]
21p	6.5[1]	30p	1.4[2]	38p	1.5[2]
22p	5.7[1]	31p	1.1[2]	39p	1.3[2]
23p	4.1[1]			40p	1.2[2]
Total	5.3[2]		1.2[3]		1.3[3]

ratios of the hydrogen density in these excited states to that in the ground state are estimated to be $N_H(n_i)/N_H(1)=0.0034$, 0.0017, and 0.000 75 for $n_i=2$, 3, and 4, respectively, for $T_e=300$ eV and $n_e=5\times10^{13}$ cm^{-3} [10].

Cascade effect of the different l distributions from $18l$ and $27l$ states to the lower levels are shown in Fig. 8 for (a) $l=0$, (b) $l=2$, (c) $l=3$, and (d) statistical weight distribution. Here $\alpha_{CE}(18l)=1.8\times10^{-7}$ and $\alpha_{CE}(27l)=6.9\times10^{-8}$ cm^{3}s^{-1} are assumed to see clearly the effect of the cascades. As we have seen in the preceding section, cascades to the lower np states from $l\geq2$ states are very small. For the statistical weight distribution, the cascade contribution is so small that the peaks of lines cannot be clearly observed.

Since the observed intensities I_{13} and I_{14} are considered to be produced mainly by radiative recombination as discussed in Sec. III B, the contribution of cascades from higher levels is expected to be small for these lines. Then for the levels with $n\geq15$ we assume that almost all of the electrons are captured to the $l=1$ state. Comparison of the modeled spectrum with the observed one is shown in Fig. 9. The cross sections derived for $n\geq15$ are listed in Table II. These cross sections are roughly expressed in the form of a Gaussian distribution as $\sigma(np)=\sigma_0\exp(-[(n-n_0)/\Delta n]^2)$, where the values of σ_0 are $68\sigma(10p)$, $180\sigma(10p)$, and $160\sigma(10p)$ and the values of Δn are 5, 6, and 8 for $n_0=19$, 27, nd 36, respectively. The populations for the levels of $n>27$ are redistributed due to l mixing. This effect is taken into account in our model calculations. The spectral lines in Fig. 9 are assumed to be emitted mainly at the plasma periphery near $r=13$ cm where $T_e\approx300$ eV, while continuum emission comes from the inner region where $T_e\approx500$ eV. This plasma is considered to be in a low-temperature recombining phase. The Boltzmann plot $N(n\,^1P)/[\omega(n\,^1P)n_ek]$ for the modeled population densities with the use of the charge exchange cross sections in Tables I and II is given in Fig. 10 from $n=3$ to 40 levels for $T_e=300$ eV, $N_e=5\times1$'0^{13} cm^{-3}, and $k=N(Ar^{17+})/N(Ar^{16+})=0.02$, where $N(n\,^1P)$ is the population density and ω the statistical weight. The population densities without charge-exchange processes and those in Saha-Boltzmann equilibrium are also shown by the dashed line and by the dotted-dashed line, respectively. The population densities would be reached in local thermodynamic equilibrium at around $n=50$. Strong population inversion is seen for the levels between $n=8$ and 10 as well as between 13 and 27. The population densities for $n\geq25$ exceed those of Saha-Boltzmann equilibrium.

IV. SUMMARY

Population inversion for $n=9$, 10, and ≥15 states found from the peripheral region of tokamak plasmas has been analyzed in terms of the charge exchange process. We have investigated the effect of cascades through charge-exchange recombination and derived charge-exchange cross sections to n-l states for the process Eq. (1) from the observed spectra. We considered the two extreme cases (A) and (B), and both fitted well to the experiment. We may assume that the actual distribution of the cross sections would be somewhere between case (A) and (B). The total cross section for $n_i=1$ is $15\sigma(10p)$ in cases (A i) and (B i), $(33-44)\sigma(10p)$ in cases (A ii) and (B ii), respectively. These values are about the same as the theoretical ones given in Ref. [6] taking the value $\sigma(10p)=4\times10^{-16}$ cm^2. The derived total cross sections from the spectra for $n_i=2$, 3, and 4 are 2.1×10^{-13}, 4.8×10^{-13}, and 5.2×10^{-13} cm^2, respectively. This result indicates a weaker n_i dependence than that proportional to n_i^4 [2,9]. The absolute values obtained in the present paper may be uncertain with an error of a factor of three depending on the uncertainties in $vN_H(1)/n_e$ in Eq. (2).

There are few theoretical and experimental studies on n-l distribution for highly ionized ions, particularly at low energies. The theoretical distributions [5–8] cannot reproduce the observed intensities from I_7 to I_{10} as mentioned in Sec. III C. The l distribution derived from the observed spectra appears to take a maximum around the s or d state for $n=9$ and 10. Since the maximum value in the s state of l distribution [(A i) and (B i)] is difficult to be expected theoretically at low energies, the second case in which the cross section increases towards the d state [(A ii) and (B ii)] would be more probable. The strong dependence on the temperature for the l distribution may exist as discussed in Sec. III. The cross sections for the g state are unknown since the effect to the np states is small. The observed spectrum for $n \geq 15$ is consistent with the l distribution having a maximum at the p state.

ACKNOWLEDGMENT

We would like to thank Professor R. K. Janev for his useful comments.

[1] E. Källne, J. Källne, A. Dalgarno, E. S. Marmar, J. E. Rice, and A. K. Pradhan, Phys. Rev. Lett. **52**, 2245 (1984).
[2] J. E. Rice, E. S. Marmar, J. L. Terry, E. Källne, and J. Källene, Phys. Rev. Lett. **56**, 50 (1986).
[3] J. E. Rice, E. S. Marmar, E. Källne, and J. Källne, Phys. Rev. A **35**, 3033 (1987).
[4] T. Fujimoto and T. Kato, Astrophys. J. **246**, 994 (1981).
[5] A. Abramov, F. F. Baryshnikov, and V. S. Lisitsa, JETP Lett. **27**, 464 (1978).
[6] R. K. Janev, D. S. Belic, and B. H. Bransden, Phys. Rev. A **28**, 1293 (1983).
[7] W. Fritsch and H. Tawara, Phys. Scr. **T28**, 58 (1989).
[8] F. Koike, J. Phys. Soc. Jpn. **57**, 2344 (1988).
[9] R. E. Olson, J. Phys. B **13**, 483 (1980).
[10] T. Fujimoto and P. McWhirter, Phys. Rev. **42**, 6588 (1990).